Aluminiums Alloy 8011

Surface Characteristics

Rahimi, Maral; Fojan, Peter; Gurevich, Leonid; Afshari, Alireza

Published in:
Applied Mechanics and Materials

DOI (link to publication from Publisher):
10.4028/www.scientific.net/AMM.719-720.29
10.4028/www.scientific.net/amm.719-720.29

Publication date:
2015

Applied Mechanics and Materials
ISSN: 1662-7482, Vols. 719-720, pp 29-37
doi:10.4028/www.scientific.net/AMM.719-720.29

Submitted: 2014-05-09
Revised: 2014-09-26
Accepted: 2014-09-26
Online: 2015-01-13

Aluminium alloy 8011:Surface characteristics

M.Rahimi[1, a], P.Fojan[2,b], L.Gurevich[3,c] and A.Afshari[4,d]

[1,4] Department of Energy and Environment, Danish Building Research Institute, Aalborg University, A.C. Meyers Vænge 15, DK-2450 Copenhagen SV, Denmark

[2,3] Department of Physics and Nanotechnology, Aalborg University, Skjernvej 4, DK-9220, Aalborg East, Denmark

[a]mar@sbi.aau.dk, [b] fp@nano.aau.dk, [c] lg@nano.aau.dk, [d] ala@sbi.aau.dk

Keywords: Aluminium alloy 8011, wettability, contact angle, roughness, frost

Abstract. Aluminium alloys are the predominant materials in modern industries. Increased knowledge about the surface characteristics of bare aluminium can enhance the understanding about how to optimize the working conditions for the equipment involving aluminium parts. This work focusses on the properties of native surface of aluminium alloy 8011, which is the main construction material for the production of air-to-air heat exchanger fins. In this study, we address its water wettability, surface roughness and frost formation in different psychometric parameters. The contact angle measurements revealed that this aluminium alloy exhibits a relatively high contact angle of about 78 degree, i.e. is not wetted completely. AFM measurements revealed significant surface roughness of typical heat exchanger fins. The thickness of formed frost was studied in relation to the wettability, humidity and the cold surface temperature.

Introduction

Aluminium alloys are the predominant materials in outdoor structures like electrical cabling, in aircraft industries and in ventilation system such as in heat exchanger production. It is widely used because of its relatively low cost, light weight, high heat conductivity and proper corrosion resistance. Aluminium alloys can be heat treated and loaded to relatively high stress levels [1][2][3].In cold conditions at temperatures below the dew point of water, formation of frost is inevitable and can cause serious malfunctions of the equipment. [4]. Aluminium alloy surface characteristics such as its roughness, contact angle and wettability play an important role for applications in cold working conditions. Frost formation and frost accretion is related to the wettability of a surface, which can be described by the contact angle that a liquid droplet form on the solid surface, is related to the surface morphology and surface chemistry[5][6][7][8].

There are two models for describing the relation between the surface morphology and the contact angle the Wenzel and Cassie-Baxter models[9][10][11].

If the liquid penetrates through the surface roughness and is in full contact with the solid surface, the contact angle is described by Wenzel's equation. On the other hand, if the water remains suspended on top of the rough surface and air is entrapped below the liquid, the contact angle is described by Cassie's state of wetting. It means that the effect of surface morphology on the contact angle is described by the Cassie-Baxter model[12].

Frost formation on the surface of aluminium alloy is an important topic of research and much significant prior research has been carried out to understand frost growth on a flat plate. In this paper, the frost formation on top of the aluminium samples in different psychrometric parameters such as air temperature, humidity and surface temperature is investigated in addition to the surface characteristics of aluminium plate samples.

Frost growth is divided into three main steps which are: crystal growth period, frost layer growth, and frost layer full-growth period. During the first stage, the ice crystals grow away from the cold surface and they are far apart and show little interaction. In the second stage, as the process continues, the crystals grow, branch out and meet together to form a layer and frost is characterised as "frost layer growth". In the "full-layer frost growth", the surface temperature of the frost reaches 0^{o}C and continuous cycles of melting and refreezing occur at this temperature which is the reason for increasing the frost layer density. These categories for frost growth are introduced first by Hayashi et al 1997 and then also observed by other researchers [13][14][15].

In frost formation and deposition on a surface psychrometric parameters such as air temperature, velocity, humidity and surface temperature have an important impact on the frost formation process, its nucleation and growth, and also on frost properties such as density and thickness[6][16][17].

Besides these psychrometric parameters, surface conditions such as surface temperature, roughness, drop adhesion to the surface and consequently the contact angle are also important parameters for frost formation [18]. It has been shown that frost formation is a heterogeneous nucleation process that is mainly influenced by the contact angle[19].Frost thickness which can block the air passage and increase the thermal resistance between air and the cold surface is the most important parameter in this frost formation study. The research results showed that the frost layer thickness increases during the frost formation process while the growing speed decreases gradually. However, it should be noted, that by increasing the air humidity or decreasing the temperatures of the cold surface and air, the frost growth can be increased[15].

Increased knowledge about the bare aluminium surface characteristics can enhance understanding how to improve working conditions for aluminium equipment and decrease manufacturing and maintenance costs. In this paper, we address surface wettability of untreated aluminium alloy 8011, which is one of the most common materials for air-to-air heat exchanger fins. To the authors' knowledge, the surface characteristics of this aluminium alloy have never been addressed in connection with its application in heat exchangers

Material

Aluminium alloy 8011 with chemical composition according to Table.1, which is used for the production of heat exchangers, was used in this study. Aluminium sheets were plain, single rolled with a thickness of 0.25 mm were cut into test samples of 15× 15 mm^2. Samples were degreased in an ultrasound cleaner in a process consisting of 10 min in an acetone bath, then 10 min in DI-water and finally 10 min in an ethanol bath. The samples were then dried under an N2 stream and put in an oven at 110 C° over night for drying.

Table 1: Chemical composition of Aluminium alloy 8011 according to EN 573-3.

Grade 8011A – content [%]										
	Si [%]	Fe [%]	Cu [%]	Mn [%]	Mg [%]	Cr [%]	Zn [%]	Ti [%]	Others each [%]	Others total [%]
min	0.40	0.50	-	-	-	-	-	-	-	-
max	0.8	1.0	0.10	0.10	0.10	0.10	0.10	0.05	0.05	0.15

Methodology

Contact angle measurement. Contact angle measurements were made by means of homemade computer-controlled sessile drops stage. Milli-Q water was supplied via a micro tube on the surface at room temperature of 24 C$^{\circ}$ with the fluid rate of 6 µL/min. The shape of contact angles were recorded by CCD camera over time and the images were interpreted and analysed by Drop Snake software (plugin for Image J software)[20]. The reported contact angle data were determined by averaging values measured at 3 different points on 4 samples.

AFM. The surface roughness morphology was measured and visualised by atomic force microscopy (NTEGRA Aura, NT-MDT Co.) in intermittent contact mode using Olympus OMCL-160TS cantilevers (Asylum Research). The RMS roughness for each group of samples was calculated as an average value of the measurements carried out over 3 areas on 3 samples. The AFM images were analysed using WSXM software [21].

Observation of the frost formation. A dedicated chamber was assembled to allow full control of the frost formation parameters, including airflow, air humidity, surrounding temperature and cold surface temperature of the test section. The experiments were performed in a clean room to ensure low concentration of polluting gases and particles. Air supply system in the clean room involved extensive air filtration using a F7-class filter, a charcoal filter followed by a second F7-class filter and finally a HEPA filter. Frost formation on the sample was monitored by a CCD camera. The recorded images were interpreted and analysed after each test and the thickness of the frost was calculated for each sample. Fig. 1shows a schematic picture of the test setup. It should be noted that due to the random nucleation on the surface, the frost layer is not flat. To account for this, several measuring techniques have been developed [22]. In the presented data, the frost thickness was measuring in at least 10 points on each sample using side images acquired with a CCD camera.

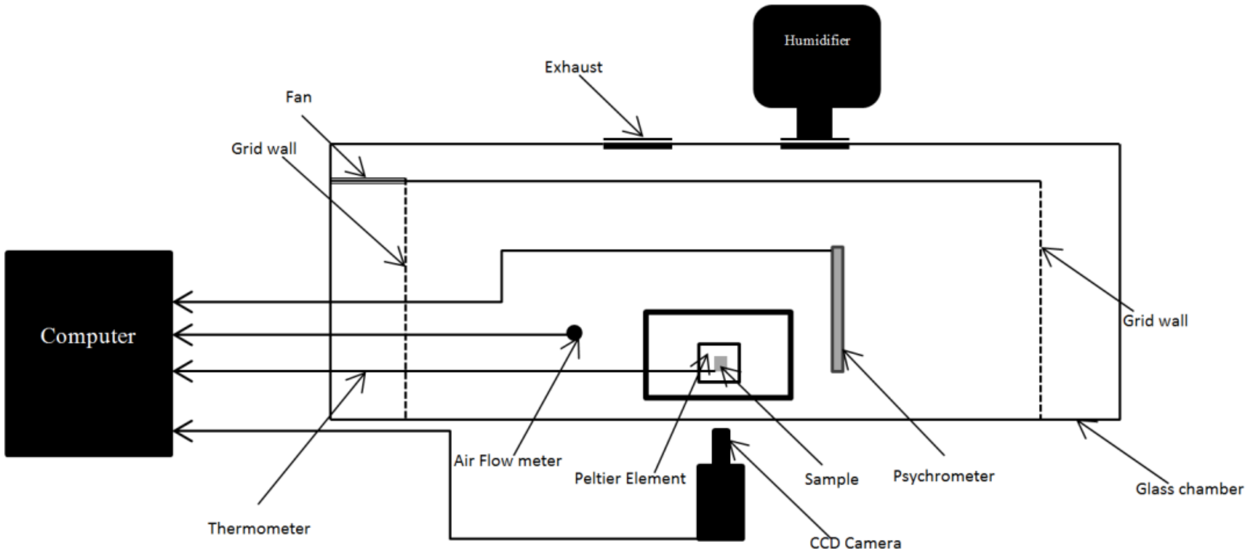

Fig.1: Schematic picture of the test setup for frost formation

Result and discussion

The measured RMS roughness of aluminium alloy samples by AFM was 84.05 nm with a 95 % confidence interval of 16.65A typical example of the observed surface morphology is shown in in Fig.2..

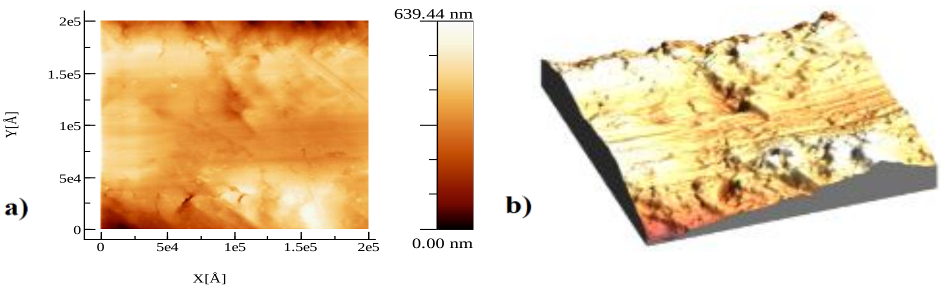

Fig.2: A typical topography of native aluminum alloy 8011 imaged with an AFM ((a) and (b) show 2D and 3D representations of the same image).

The contact angle measurement on the surface of the samples showed that the water drop forms a contact angle of 78° on the untreated surface of aluminium alloy 8011.The measured amount is a significantly high contact angel since aluminium alloys are considered to be high surface-energy materials and they were expected to be hydrophilic with a low contact angle and be completely wetted. This can be explained by the fact that the exposure of aluminium surface to the atmosphere causes hydrophobic organic contamination and hence the water contact angle on its surface is increased. This observation was in line with the other observations and also in line with other clean metal surfaces,[23][24].Due to its high roughness and the air pocket structure in its surface, it follows the Cassie-Baxtermodel and has a large contact angle. The rough surface of aluminium entraps air in the gaps and forms a composite surface of air and solid material. The entrapped air under the liquid reduces the interfacial contact area between the solid surface and the liquid which leads to a higher water contact angle[5][25][23][24].

On the other hand, such a rough and inhomogeneous surface also leads to the pinning of the contact line during evaporation of the droplet. Fig.3shows that the three-phase contact line remained pinned and that the contact angle decreased constantly after the initial stage of evaporation with a constant advancing contact angle. A similar phenomenon has been observed by Shanahan and Bourgès-Monnier who noted that the surface roughness makes it impossible to introduce a specific value of the receding contact angle due to the constant decrease of the contact angle and the height of droplet till the moment of total evaporation of the droplet[26]. Bormashenko et al. also observed this phenomenon on aluminium and steel surfaces [24].

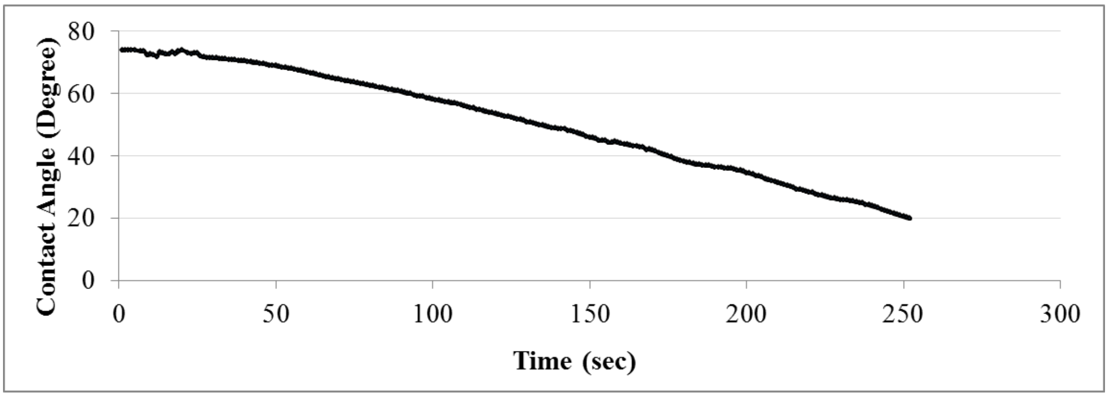

Fig.3: Receding contact angle of an evaporating sessile drop on the surface of aluminium alloy 8011

The thickness of the frost formed on top of the aluminium alloy samples after 5 and 10 min is shown in Fig.4 for three different values of relative humidity. As, it can be seen at a constant humidity, the frost thickness increases over time.

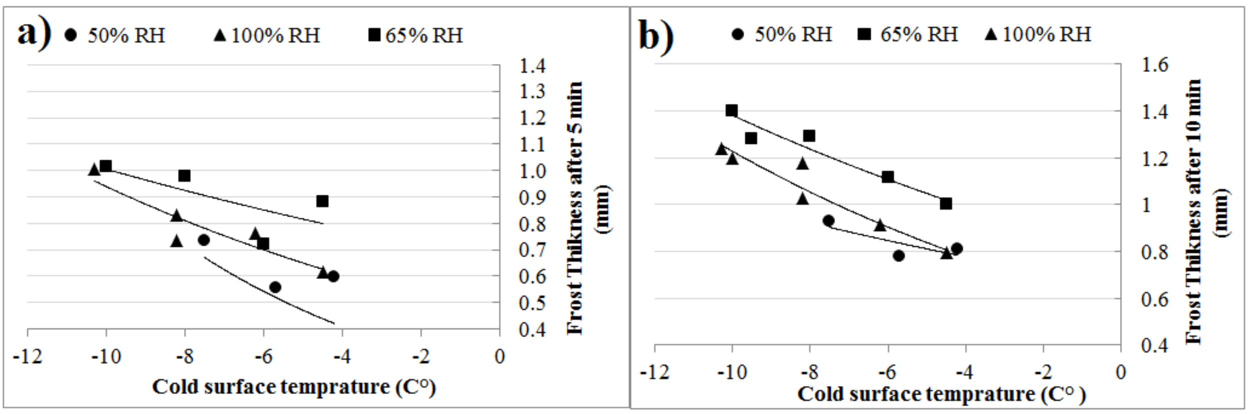

Fig.4: Thickness of the frost formed on top of the samples after a) 5 min and b)10 min at different humidity

The density of the formed frost at relative humidity of 50%, 65% and 100% is shown in Fig.5.It can be seen that the frost density decreased upon decrease in cold surface temperature. This observation is in line with previous works and researches [27][13][22].

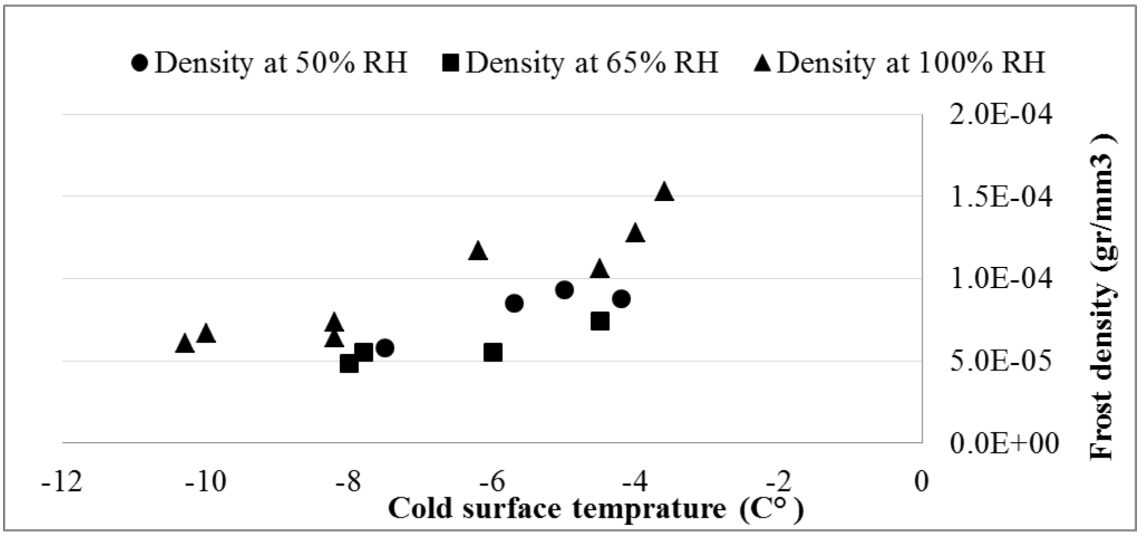

Fig.5: The density of formed frost on top of the samples at different humidity

Fig.6 shows that the frost formation can indeed be divided into three main stages. In the beginning of process, individual ice crystals nucleate on the cold surface(see Fig.6.a),then these crystalsgrow, with approximately the same rate, in a direction perpendicular to the surface, see Fig.6.b. Over time, the crystals branched out, collide and grew in a direction parallel to the surface direction forming a layer of frost, seeFig.6.c. This observation was in line with the steps that reported by Hayashi et al. (1977).

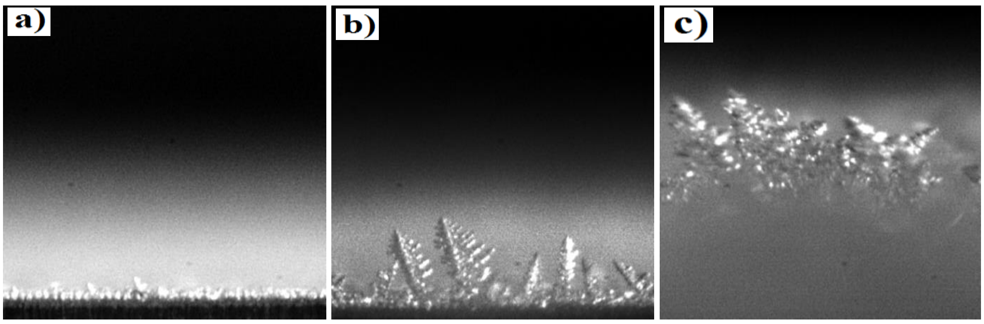

Fig.6: Frost formation images at a humidity of 65% and at -8 C° a) in the beginning nucleation, b) after 5 min, and c) after 10 min viewed from the edge of aluminum plate

Fig.7 shows that increasing the humidity of the air stream clearly increased the frost deposition rate Since by increasing the humidity the mass transfer rate will be increased and the mass of deposited frost will be increased.

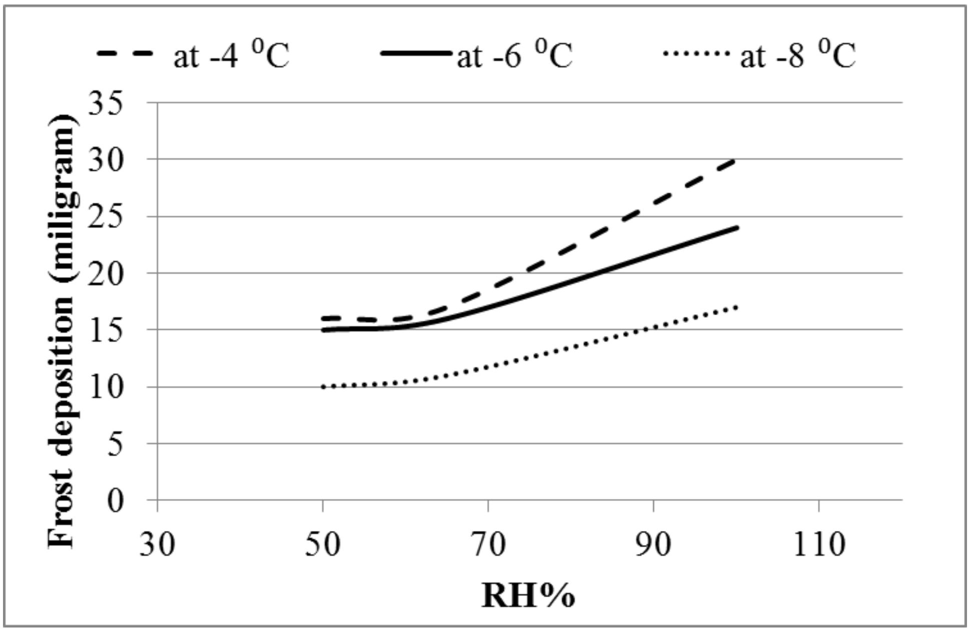

Fig.7: Frost deposition (milligram) at different humidity and cold surface temperatures

Conclusion

The studies of wetting characteristics of the native surface of aluminium alloy 8011 revealed that this surface exhibit a relatively high contact angle of 78 °C. This result can be explained by a significant roughness of the native surface of the alloy (shown by AFM measurements) in combination with inevitable surface contaminations common for high-energy metal surfaces. As we found in our previous publication [5].Such a combination of parameters should lead to Cassie-Baxter behaviour, where the interface between the water droplet and aluminium includes patches of trapped air. In this case a simple further roughening of the surface can make it stably hydrophobic which may be essential for alloy application in heat exchangers and outdoor equipment. Our measurements also provide an insight into the receding behaviour of water droplet on the alloy. It was observed that upon drying of a droplet the three-phase contact line remained pinned and the contact angle decreased constantly. Further, this paper experimentally studied the local frost formation process on a cold surface of aluminium alloy 8011 at different air humidityand cold surface temperatures.

References

[1] E.A. Starke, J.T. Staleyt, Application of modern alluminum alloys to aircraft, Prog. Aerosp. Sci. 32 (1996) 131–172.

[2] T. Dursun, C. Soutis, Recent developments in advanced aircraft aluminium alloys, Mater. Des. 56 (2014) 862–871.

[3] W. Zhang, D. Zhang, Y. Le, L. Li, B. Ou, Fabrication of surface self-lubricating composites of aluminum alloy, Appl. Surf. Sci. 255 (2008) 2671–2674.

[4] R. Menini, Z. Ghalmi, M. Farzaneh, Highly resistant icephobic coatings on aluminum alloys, Cold Reg. Sci. Technol. 65 (2011) 65–69.

[5] M. Rahimi, P. Fojan, L. Gurevich, A. Afshari, Effects of aluminium surface morphology on wettability and roughness, Appl. Surf. Sci. 2014, http//dx.doi.org/doi10.1016/j.apsusc.2014.01.059.

[6] C.J.L. Hermes, An analytical solution to the problem of frost growth and densification on flat surfaces, Int. J. Heat Mass Transf. 55 (2012) 7346–7351.

[7] A. Bayer, J.J. Schrijder, The Wettability of Industrial Surfaces : Contact Angle Measurements and Thermodynamic Analysis, 19 (1985) 277–285.

[8] M.K. Kwak, H.-E. Jeong, T. Kim, H. Yoon, K.Y. Suh, Bio-inspired slanted polymer nanohairs for anisotropic wetting and directional dry adhesion, Soft Matter. 6 (2010) 1849.

[9] R.N. Wenzel, Resistance of solid surfaces, Ind. Eng. Chem. 28 (1936) 988–994.

[10] A.B.D. Cassie, S. Baxter, Wettability of porous surfaces, Trans. Faraday Soc. 40 (1944) 546–551., Trans. Faraday Soc. 40 (1944) 546–551.

[11] a J.B. Milne, a Amirfazli, The Cassie equation: how it is meant to be used., Adv. Colloid Interface Sci. 170 (2012) 48–55.

[12] C. Dorrer, J. Rühe, Drops on microstructured surfaces coated with hydrophilic polymers: Wenzel's model and beyond, Langmuir. 24 (2008) 1959–64.

[13] Y. Hayashi, A. Aoki, S. Adashi, K. Hori, Study of frost properties correlating with frost formation types, ASME J. Heat Transf. 99 (1977) 239–245.

[14] K.S. Lee, W.S. Kim, T.H. Lee, A one-dimensional model for frost formation on a cold flat surface, Int. J. Heat Mass Transf. 40 (1997) 4359–4365.

[15] K. Qu, S. Komori, Y. Jiang, Local variation of frost layer thickness and morphology, Int. J. Therm. Sci. 45 (2006) 116–123.

[16] K.S. Lee, S. Jhee, D.-K. Yang, Prediction of the frost formation on a cold flat surface, Int. J. Heat Mass Transf. 46 (2003) 3789–3796.

[17] W. Wang, Q.C. Guo, W.P. Lu, Y.C. Feng, W. Na, A generalized simple model for predicting frost growth on cold flat plate, Int. J. Refrig. 35 (2012) 475–486.

[18] R. Tadmor, P. Bahadur, A. Leh, H.E. N'guessan, R. Jaini, L. Dang, Measurement of Lateral Adhesion Forces at the Interface between a Liquid Drop and a Substrate, Phys. Rev. Lett. 103 (2009) 26610-1–26610-4.

[19] B. Na, R.L. Webb, A fundamental understanding of factors affecting frost nucleation, Int. J. Heat Mass Transf. 46 (2003) 3797–3808.

[20] M.D. Abràmoff, P.J. Magalhães, S.. Ram, Image Processing with ImageJ, Biophotonics Int. 11 (2004) 36–42.

[21] I. Horcas, R. Fernández, J.M. Gómez-Rodríguez, J. Colchero, J. Gómez-Herrero, a M. Baro, WSXM: a software for scanning probe microscopy and a tool for nanotechnology., Rev. Sci. Instrum. 78 (2007) 013705-1–013705-9.

[22] I. Tokura, H. Saito, K. Kishinami, Study on properties and growth rate of frost layers on cold surface.pdf, Trans. ASME,J. Heat Transf. 105 (1983) 895–901.

[23] W.A. Zisman, K.W. Bewig, The Wetting of Gold and Platinum by Water, J. Phys. Chem. 1097 (1966) 4238–4242.

[24] E. Bormashenko, A. Musin, M. Zinigrad, Evaporation of droplets on strongly and weakly pinning surfaces and dynamics of the triple line, Colloids Surfaces A Physicochem. Eng. Asp. 385 (2011) 235–240.

[25] S.H. Kim, Fabrication of Superhydrophobic Surfaces, J. Adhes. Sci. Technol. 22 (2008) 235–250.

[26] M.E.R. Shanahan, C. Bourg, Effects of evaporation on contact angles on polymer surfaces, Int. J. Adhes. Adhes. 14 (3) (1994) 201–205.

[27] C.-H. Cheng, Y.-C. Cheng, Prediction of frost groeth on a cold plate in atmospheric air, Int. Comm. Heat Mass Transf. 28 (2001) 953–962.

Materials and Engineering Technology
10.4028/www.scientific.net/AMM.719-720

Aluminium Alloy 8011: Surface Characteristics
10.4028/www.scientific.net/AMM.719-720.29

DOI References
[1] E.A. Starke, J.T. Staleyt, Application of modern alluminum alloys to aircraft, Prog. Aerosp. Sci. 32 (1996) 131-172.
10.1016/0376-0421(95)00004-6
[2] T. Dursun, C. Soutis, Recent developments in advanced aircraft aluminium alloys, Mater. Des. 56 (2014) 862-871.
10.1016/j.matdes.2013.12.002
[3] W. Zhang, D. Zhang, Y. Le, L. Li, B. Ou, Fabrication of surface self-lubricating composites of aluminum alloy, Appl. Surf. Sci. 255 (2008) 2671-2674.
10.1016/j.apsusc.2008.07.209
[4] R. Menini, Z. Ghalmi, M. Farzaneh, Highly resistant icephobic coatings on aluminum alloys, Cold Reg. Sci. Technol. 65 (2011) 65-69.
10.1016/j.coldregions.2010.03.004
[6] C.J.L. Hermes, An analytical solution to the problem of frost growth and densification on flat surfaces, Int. J. Heat Mass Transf. 55 (2012) 7346-7351.
10.1016/j.ijheatmasstransfer.2012.06.070
[8] M.K. Kwak, H. -E. Jeong, T. Kim, H. Yoon, K.Y. Suh, Bio-inspired slanted polymer nanohairs for anisotropic wetting and directional dry adhesion, Soft Matter. 6 (2010) 1849.
10.1039/b924056j
[9] R.N. Wenzel, Resistance of solid surfaces, Ind. Eng. Chem. 28 (1936) 988-994.
10.1021/ie50320a024
[10] A.B.D. Cassie, S. Baxter, Wettability of porous surfaces, Trans. Faraday Soc. 40 (1944) 546- 551., Trans. Faraday Soc. 40 (1944) 546-551.
10.1039/tf9444000546
[11] a J.B. Milne, a Amirfazli, The Cassie equation: how it is meant to be used., Adv. Colloid Interface Sci. 170 (2012) 48-55.
10.1016/j.cis.2011.12.001
[12] C. Dorrer, J. Rühe, Drops on microstructured surfaces coated with hydrophilic polymers: Wenzel's model and beyond, Langmuir. 24 (2008) 1959-64.
10.1021/la7029938
[13] Y. Hayashi, A. Aoki, S. Adashi, K. Hori, Study of frost properties correlating with frost formation types, ASME J. Heat Transf. 99 (1977) 239-245.
10.1115/1.3450675
[14] K.S. Lee, W.S. Kim, T.H. Lee, A one-dimensional model for frost formation on a cold flat surface, Int. J. Heat Mass Transf. 40 (1997) 4359-4365.
10.1016/S0017-9310(97)00074-4
[15] K. Qu, S. Komori, Y. Jiang, Local variation of frost layer thickness and morphology, Int. J. Therm. Sci. 45 (2006) 116-123.
10.1016/j.ijthermalsci.2005.05.004

[16] K.S. Lee, S. Jhee, D. -K. Yang, Prediction of the frost formation on a cold flat surface, Int. J. Heat Mass Transf. 46 (2003) 3789-3796.
10.1016/S0017-9310(03)00195-9
[17] W. Wang, Q.C. Guo, W.P. Lu, Y.C. Feng, W. Na, A generalized simple model for predicting frost growth on cold flat plate, Int. J. Refrig. 35 (2012) 475-486.
10.1016/j.ijrefrig.2011.10.011
[18] R. Tadmor, P. Bahadur, A. Leh, H.E. N'guessan, R. Jaini, L. Dang, Measurement of Lateral Adhesion Forces at the Interface between a Liquid Drop and a Substrate, Phys. Rev. Lett. 103 (2009) 26610-1-26610-4.
10.1103/PhysRevLett.103.266101
[19] B. Na, R.L. Webb, A fundamental understanding of factors affecting frost nucleation, Int. J. Heat Mass Transf. 46 (2003) 3797-3808.
10.1016/S0017-9310(03)00194-7
[21] I. Horcas, R. Fernández, J.M. Gómez-Rodríguez, J. Colchero, J. Gómez-Herrero, a M. Baro, WSXM: a software for scanning probe microscopy and a tool for nanotechnology., Rev. Sci. Instrum. 78 (2007) 013705-1-013705-9.
10.1063/1.2432410
[22] I. Tokura, H. Saito, K. Kishinami, Study on properties and growth rate of frost layers on cold surface. pdf, Trans. ASME,J. Heat Transf. 105 (1983) 895-901.
10.1115/1.3245679
[24] E. Bormashenko, A. Musin, M. Zinigrad, Evaporation of droplets on strongly and weakly pinning surfaces and dynamics of the triple line, Colloids Surfaces A Physicochem. Eng. Asp. 385 (2011) 235-240.
10.1016/j.colsurfa.2011.06.016
[25] S.H. Kim, Fabrication of Superhydrophobic Surfaces, J. Adhes. Sci. Technol. 22 (2008) 235- 250.
10.1163/156856108X305156
[26] M.E.R. Shanahan, C. Bourg, Effects of evaporation on contact angles on polymer surfaces, Int. J. Adhes. Adhes. 14 (3) (1994) 201-205.
10.1016/0143-7496(94)90031-0
[27] C. -H. Cheng, Y. -C. Cheng, Prediction of frost groeth on a cold plate in atmospheric air, Int. Comm. Heat Mass Transf. 28 (2001) 953-962.
10.1016/S0735-1933(01)00299-8